Fluid Dynamics & Materials Processing

Tech Science Press

DOI: 10.32604/fdmp.2023.045260

REVIEW

Hydrodynamic Cavitation Enhanced SR-Aops Degradation of Organic Pollutants in Water: A Review

Xiufeng Zhu[1,2] and Jingying Wang[1,*]

[1]School of Energy and Power Engineering, Shandong University, Jinan, 250061, China

[2]Key Laboratory of High Efficiency and Clean Machinery Manufacturing of Ministry of Education, School of Mechanical Engineering, Shandong University, Jinan, 250061, China

[*]Corresponding Author: Jingying Wang. Email: wjy_sdu@sdu.edu.cn

Received: 21 August 2023 Accepted: 01 December 2023 Published: 28 March 2024

ABSTRACT

SR-AOP (sulfate radical advanced oxidation process) is a novel water treatment method able to eliminate refractory organic pollutants. Hydrodynamic cavitation (HC) is a novel green technology, that can effectively produce strong oxidizing sulfate radicals. This paper presents a comprehensive review of the research advancements in these fields and a critical discussion of the principal factors influencing HC-enhanced SR-AOP and the mechanisms of synergistic degradation. Furthermore, some insights into the industrial application of HC/PS are also provided. Current research shows that this technology is feasible at the laboratory stage, but its application on larger scales requires further understanding and exploration. In this review, some attention is also paid to the design of the hydrodynamic cavitation reactor and the related operating parameters.

KEYWORDS

Hydrodynamic cavitation; organic pollutant; persulfate; degradation; influence factor

Nomenclature

HC	Hydrodynamic cavitation
PS	Persulfate
SR-AOP	Sulfate radical advanced oxidation process
HCRs	Hydrodynamic cavitation reactors
GPD	A glow plasma discharge system
SIS	Scrap iron sheet
ED	Decolorization

1 Introduction

Rapid development of industrialization has led to substantial growth in key sectors, including pharmaceuticals, chemicals, printing, dyeing, and paper production. Consequently, there has been a notable increase in the volume of industrial wastewater which exhibits complex composition and poor biodegradability. These highly toxic and resistant organic pollutants pose a grave threat to the ecological integrity of water environments and the well-being of individuals [1,2].

At present, the conventional treatment methods for this wastewater include physical methods [3], chemical methods [4], and biological methods [5]. However, physical methods (gas flotation method, extraction method, and precipitation method) usually separate the pollutants from water and are not suitable for the deep degradation of organic wastewater [4]. Biological methods (anaerobic method, aerobic method, and anaerobic-aerobic combination method [6]) are associated with lengthy treatment time, extensive equipment area requirements, stringent operating environment conditions, and limited efficacy in treating wastewater with low biodegradability [7]. Chemical methods (chlorine oxidation, ozone oxidation, Fenton oxidation, photocatalytic oxidation, and low-temperature plasma oxidation) have the potential to induce secondary pollution of water [8]. Therefore, the development of novel and efficient environmentally friendly treatment technologies for organic pollutant wastewater is of great social significance and economic value.

Some scholars have found that the advanced oxidation process offers a water treatment method that can rapidly mineralize most recalcitrant organic pollutants into carbon dioxide, water, and af inorganic salts [9]. It usually refers to an oxidation technology involving hydroxyl radical (•OH) parameters [10]. SR-AOP is a novel approach that has just emerged in recent years which uses sulfate radical (SO_4^{-}•) to degrade persistent organic pollutants. Compared with traditional advanced oxidation processes, it has the characteristics of more oxidant stability, longer half-life, higher oxidation-reduction potential of key free radicals, and less pH dependence, which are conducive to the degradation of pollutants [11]. The specific data is shown in Table 1. However, persulfate (PS) is stable at room temperature and has limited degradation effectiveness towards pollutants. Therefore, a series of activation methods for PS has been developed to generate strongly oxidizing sulfate radicals. The main approaches of activation are shown in Fig. 1, including thermal activation [12], transition metal ion activation [13], cavitation activation [14], ultraviolet activation [15], alkali activation [16], and ultrasound activation [17]. Among them, the hydrodynamic cavitation (HC) activated persulfate (PS) synergistic degradation technique proposed by Choi et al. [18] in 2018 has attracted much attention for its remarkable efficiency, cost-effectiveness, and wide applicability.

Table 1: The comparison of •OH and SO_4^{-}•

Radical	Oxidation potential	Oxidant stability	Half-life	Effects of pH
SO_4^{-}•	+2.60 − +3.10 V	Stable	4 s	Independent
•OH	+1.90 − +2.70 V	Loss in the form of gas and heat	~1 ns	Dependent

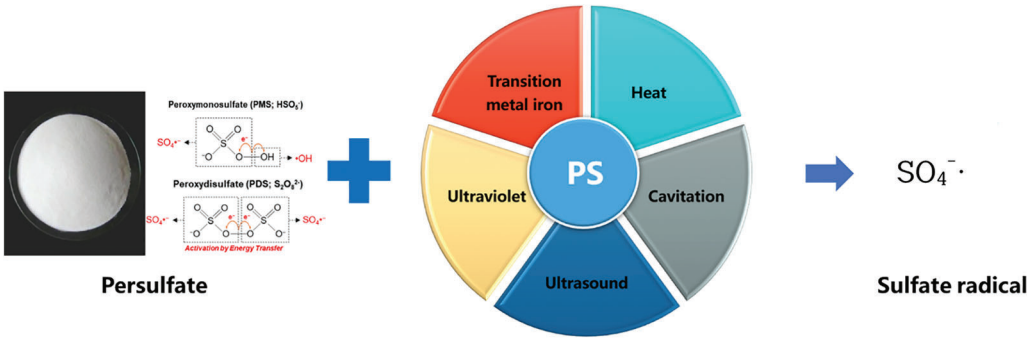

Figure 1: The main activation methods of PS

Hydrodynamic cavitation is a promising method for process intensification and has gained significant attention recently [19]. It exhibits remarkable efficiency in degrading persistent organic pollutants while being environmentally friendly and able to work in concert with a variety of physical and chemical methods. Furthermore, compared with emerging technologies such as ultrasonic, photocatalysis, and microwave, HC has the advantages of low equipment cost, facile process scalability, convenient installation, and simplicity and convenience of use [20].

At present, although water treatment teams led by Lakshmi et al. [21,22] have been formed, the research on water treatment based on the HC/PS system is still in the initial stage and the degradation mechanism of HC/PS system needs to be further explored. Considering the significant potential applications of HC/PS technology in organic pollutant degradation, this paper focuses on the research progress of HC and its enhancement mechanism, the progress of HC/PS systems in degrading water pollutants, and the key factors affecting its degradation efficiency. Additionally, the future development direction of the system is also predicted to promote the understanding of the technology among domestic researchers, to provide insights for the investigation of cavitation-enhanced persulfate degradation of water pollutants, and to establish a foundation for expediting the rapid development and application of HC/PS technology.

2 Hydrodynamic Cavitation and Its Strengthening Mechanism

2.1 Cavitation Phenomenon and Cavitation

The cavitation phenomenon [23] is a process in which the gas nuclei in the liquid grow and collapse in a very short time, generally accompanied by a large energy release (Fig. 2). It occurs when the internal pressure of the liquid drops sharply below the saturated vapor pressure due to the sharpness of the flow path or the input of external energy. The specific manifestation of this energy is a combination of physical effects (mechanical and thermal) and chemical effects.

Mechanical effects: The collapse of bubbles caused by cavitation led to significant changes in the gas-liquid interface within a very short time, resulting in strong shear stress of up to 3.5 kPa within 3 μs [24], shock waves with an average propagation velocity of 2000 m/s within 34 ns [25], microjets exceeding 160 m/s but not higher than 200 m/s, and water hammer pressures of 200 MPa [26]. These powerful mechanical effects have multiple impacts on the system. Firstly, they can intensify turbulence within the fluid and enhance mixing between the reactants. Secondly, they lead to the breaking of macromolecular carbon chains and cause organic macromolecules to break into smaller organic molecules. Finally, they possess the capability to destroy the large π bonds in graphite layers, thus weakening the strong van der Waals forces that maintain the cohesion of these layers.

Thermal effect: When a bubble collapses, a local “hot spot” is formed in the bubble, causing the temperature to rise to 5200 K. Furthermore, the heating and cooling rate of the nearby liquid exceeds 10^{10} K/s [27], which is conducive to the thermal decomposition of organic substances. The thermal and mechanical effects of cavitation can increase the mass and heat transfer processes at the reaction interface as well as the vortex effect.

Chemical effect: Under the extremely high temperatures and pressures described above, the decomposition of water molecules occurs, generating strongly oxidized •OH and H_2O_2 with strong oxidation [28], which can lead to non-selective mineralization of pollutants.

Some chemical processes such as extraction, leaching, adsorption, absorption, crystallization, emulsification, demulsification, membrane processes, descaling, degassing, defoaming, filtration, condensation sedimentation, suspension separation, oil recovery, solid particle crushing, heat transfer, and ultrasonic cleaning predominantly rely on the physical effects of cavitation phenomena. The chemical effects of cavitation are mainly used in the synthesis or degradation of organic matter, electrochemistry, and homogeneous and heterogeneous chemical reactions.

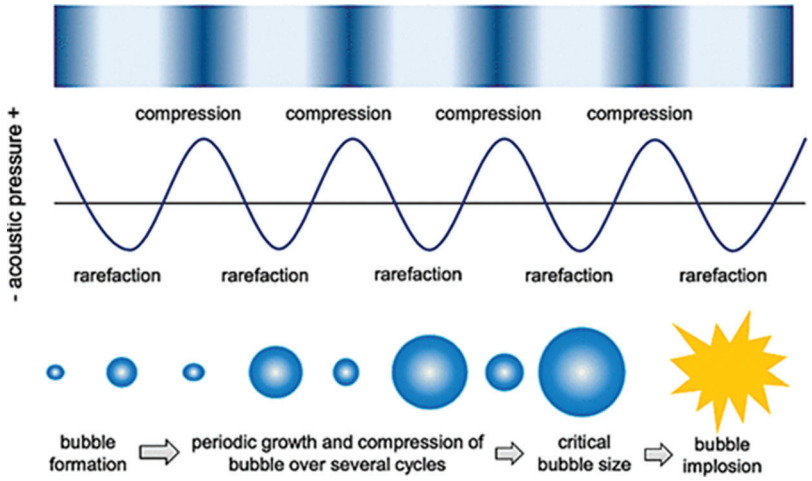

Figure 2: Cavitation phenomenon: The process of growth and collapse of cavitation bubbles. Adapted with permission from reference [29]. Copyright © 2021, License MDPI

The physical and chemical effects caused by cavitation mentioned above can generally be divided into three reaction regions according to the different regions where they occur [30], as shown in Fig. 3.

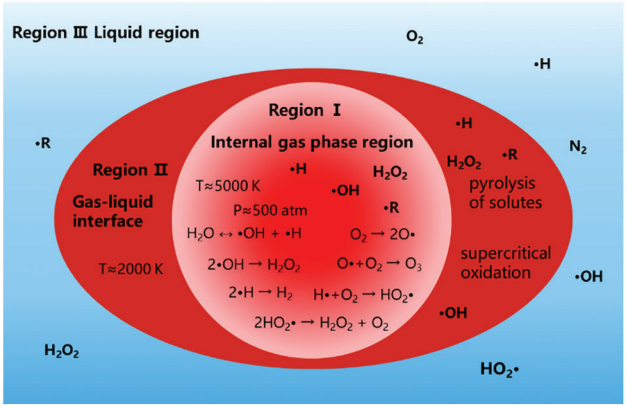

Figure 3: Three reaction regions in the cavitation process

(1) Internal gas phase region (the area within the cavitation bubble): This is the center of "hot spot", where the reactants are the medium liquid and the vapors of volatile substances with vapor pressures similar to those of the medium liquid. The extremely high temperature and high pressure generated here can cause the acoustic dissociation of water molecules into •OH and •H and also supply activation energy for bond breaking. Moreover, the resultant free radicals can react with each other to generate new molecules and new free radicals or diffuse into the solution as oxidizing agents to continue participating in other reactions.

(2) Gas-liquid interface: The temperature here can be heated to 2000 K by the core. Transient supercritical water and high concentrations of •OH and •H here result in supercritical oxidation reactions [31]. In addition, the collapse of the cavity induces a drastic change at the interface, which greatly facilitates the mixing of the reactants and an emulsification effect can be achieved for heterogeneous reactants.

(3) Liquid region: The pressure and temperature in this region are returned to environmental conditions. The reaction with the contaminants is mainly the reactive substances formed in the regions I and II.

2.2 Hydrodynamic Cavitation and Hydrodynamic Cavitation Reactors

HC is induced by the large pressure difference that occurs when a fluid passes through a specific hydraulic structure (venturi, orifice plate, etc.). This pressure difference leads to the formation and collapse of bubbles. Currently, the hydrodynamic cavitation reactors (HCRs) encompass two main types: the non-rotary cavitation reactor and the rotary cavitation reactor [32].

The most commonly used types of non-rotary HCRs in various applications are venturi, orifice plate, and vortex diode (Figs. 4a, 4b) [33]. The operational principle of Non-rotational HCRs is based on the principle of conservation of mass and Bernoulli's theorem. As the liquid passes through the constricted portion of the device, the flow rate of the fluid increases and the pressure decreases. When its internal pressure is at or below the saturation vapor pressure of the liquid, it causes gas nuclei in the liquid to form cavitation bubbles within a very short period. When the cavitation bubble flows with the fluid toward the divergence region, it collapses as the pressure recovers dramatically, generating a tremendous amount of energy as it collapses. This type of HCR does not require internal assembly or moving parts. Its simple structure makes it easy to manage and use.

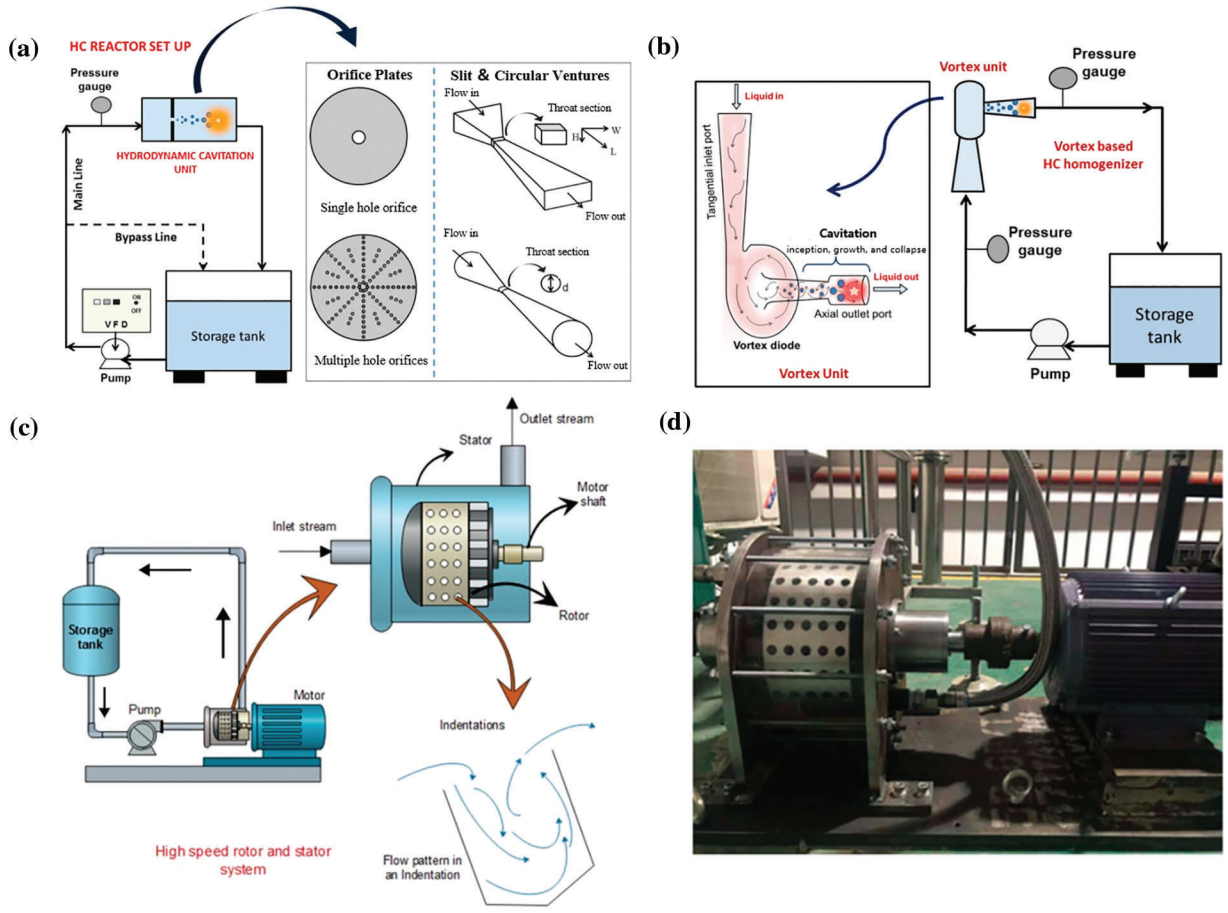

Figure 4: Representative HCRs: (a) Venturi or orifice plate HCR [34], (b) vortex type HCR [34], (c,d) rotational HCR [34,35]. Adapted with permission from reference [34], Copyright © 2022, American Chemical Society. Reference [35], Copyright © 2022, Zhang, Xie, Fan and Liu. This is an open-access article distributed under the terms of the Creative Commons Attribution License (CC BY)

The key part of rotary HCRs is the stator and rotor (Figs. 4c, 4d). HC is induced by the rapid speed shear of the fluid through blind holes on the rotor. Vacuole is periodically generated and collapsed, thus significantly improving the efficiency of cavity collapse and energy release. This mechanism facilitates the mixing of oxidizing substances and the improvement of reaction kinetics, thus enhancing the overall performance of the system [34].

2.3 Application of HC in the Degradation of Organic Pollutants

The chemical effects of HC can degrade organic pollutants in water by non-selective oxidation; the thermal effects can cause the pyrolysis reaction of pollutants; mechanical effects can destroy the main chain of macromolecules and break them into smaller molecules. In addition, the jets and shock waves produced by cavitation collapse can bring •OH and •H into the whole solution system, accelerating the mixing of reactants, and thus improving the degradation rate of organic pollutants. Furthermore, the enormous energy released by cavitation can provide the necessary energy for the reaction.

In 1993, Joshi et al. [36] conducted experiments on the hydrolysis of castor oil and safflower oil by HC and found that at the same degree of hydrolysis, the energy consumption of HC was lower than that of traditional ultrasonic cavitation, thus kicking off the degradation of pollutants by HC. In 2001, Sivakumar et al. [37] concluded that HC has great advantages in terms of magnification based on the comparative experiments between HC and ultrasonic cavitation for the degradation of Rhodamine B, because HC can effectively degrade 50 L wastewater under simple operating conditions, whereas ultrasonic cavitation can only treat tens of milliliters of wastewater. In the same operating conditions to treat Rhodamine B wastewater, the efficiency of HC is 2 times that of ultrasonic cavitation. Table 2 lists the representative studies on the degradation of pollutants by HC. In addition to its standalone application, HC exhibits notable compatibility with diverse methods, including hydrogen peroxide, ozone, Fenton, photocatalysis, persulfate, and others. Collaborative treatment not only greatly enhances the degradation efficacy (the degradation effect of collaborative treatment is several times the sum of the effect of single use), but also substantially reduces reaction time. Additionally, the system exhibits remarkable amplification, thereby showing outstanding industrial application prospects.

Table 2: Representative studies on the degradation of pollutants by HC

Year	Compounds	Process	HCR	Operational condition	Time (min)	Degradation	Ref.
2000	P-nitrophenol	HC	Otifice	P_{in} = 0.48 MPa, $C_{initial}$ = 8 ppm, $T_{initial}$ = 42°C, pH = 4.8	240	HC: 95%	[38]
2006	Phenol	HC/O_3	Orifice	P_{in} = 0.45 MPa, $C_{initial}$ = 10 mg/L, $T_{initial}$ = 50°C, pH = 3, C_{O_3} = 2.26 mg/L	60	HC: 20.6%; HC/O_3: 73.6%	[39]
2009	Alachlor	HC	Orifice	P_{in} = 0. 6 MPa, $C_{initial}$ = 50 mg/L, $T_{initial}$ = 40°C, pH = 12	100	HC: 82.3%	[40]

(Continued)

Table 2 (continued)

Year	Compounds	Process	HCR	Operational condition	Time (min)	Degradation	Ref.
2011	Acid Red 88	HC/H_2O_2	Venturi	P_{in} = 5 bar, $C_{initial}$ = 0.1 mM, $T_{initial}$ = 35°C, pH = 2, $C_{H_2O_2}$ = 4 mM	120	HC: 35.7% (TOC); HC/H_2O_2: 71.42% (TOC)	[41]
2013	Rhodamine B	HC/SIS	Orifice	P_{in} = 5.8 bar, $C_{initial}$ = 2 mg/L, $T_{initial}$ = 25°C, pH = 3, C_{O_2} = 2 L/min, $C_{Fe^{2+}}$ = 0.213 mM	240	HC/SIS: 87% (ED)	[42]
2014	Imidacloprid	HC/H_2O_2	Venturi	P_{in} = 4 bar, $C_{initial}$ = 20 ppm, $T_{initial}$ = 34°C, pH = 3, $C_{H_2O_2}$ = 20 mg/L	120	HC: 23.85%; HC/H_2O_2: 99.14%	[43]
2016	Blue 13	HC/O_2/Fe^{2+}	Orifice	P_{in} = 0.4 MPa, $C_{initial}$ = 30 ppm, $T_{initial}$ = 30°C, pH = 2, SIS = 20 g	120	HC: 47.47% (ED); HC/O_2: 65% (ED); HC/Fe^{2+}: 66.3% (ED)	[44]
2017	2,4,6-trichlorophenol	HC/O_3	Venturi	P_{in} = 4 bar, $C_{initial}$ = 20 ppm, $T_{initial}$ = 30°C, pH = 7, C_{O_3} = 400 mg/h	120	HC: 24.34%; HC/O_3: 97.11%	[45]
2017	Rhodamine B	HC/ Fenton	Venturi	P_{in} = 10 MPa, $C_{initial}$ = 33 mg/L $T_{initial}$ = 26°C, pH = 3, Fenton (H_2O_2: 30 mg/L, $FeSO_4$: 5 mg/L)	120	HC: 24.34%; HC/Fenton: 99.72%	[46]
2017	Tetracycline	HC/UV	Venturi	P_{in} = 0.34 MPa, $C_{initial}$ = 30 mg/L, $T_{initial}$ = 30°C, pH = 4.2, C_{TiO_2} = 100 mg/L	150	HC: 20.39%; HC/UV: 86.52%	[47]
2018	Bisphenol A	HC/PS	Orifice	P_{in} = 0.5 MPa, $C_{initial}$ = 0.044 mM, $T_{initial}$ = 50°C, pH = 6, C_{PS} = 0.7 mM	120	HC: 11.31%; HC/PS: 78.22%	[18]
2020	Benz[a] anthracene	HC/ClO_2	Orifice	P_{in} = 4 bar, $C_{initial}$ =5 μg/L, $T_{initial}$ = 34°C, pH = 2, C_{ClO_2} = 25 mg/L	120	HC: 45.7%; HC/ClO_2: 98.8%	[48]

(Continued)

Table 2 (continued)

Year	Compounds	Process	HCR	Operational condition	Time (min)	Degradation	Ref.
2020	Brilliant cresyl blue	HC/H_2O_2/PS	Venturi	P_{in} = 1.7 bar, $C_{initial}$ = 5 mg/L, T = 20°C, pH = 7. $C_{H_2O_2}$ = 0.22 mL/min, C_{PS} =1 M	120	HC: 10% HC/H_2O_2: 96.49%; HC/PS: 98.47%	[49]
2022	Metformin	HC/H_2O_2	Vortex	P_{in} = 1 bar, $C_{initial}$ = 10 mg/L, $T_{initial}$ = 35–40°C, pH = 4, $C_{H_2O_2}$ = 5 g/l	180	HC: 95%; HC/H_2O_2: 100	[50]
2023	Metronidazole	HC/GPD	Orifice	P_{in} = 70 bar, $C_{initial}$ = 300 mM, $T_{initial}$ = 14°C, pH = 5.8, Discharge voltage = 15 kV	15	HC: 14%; HC/GPD: 90%	[51]

3 Sulfate Radical-Based Advanced Oxidation Processes

This technology effectively degrades organic pollutants by using several methods to activate sulfate to generate sulfate ($SO_4^{\bullet-}$). Currently, the commonly used persulfates in wastewater treatment are peroxymonosulfate and peroxodisulfate [11], which play a crucial role in the oxidation process by generating $SO_4^{\bullet-}$.

The degradation of organic pollutants by PS occurs mainly through two mechanisms: direct mineralization of pollutants via hydrolysis of PS to $S_2O_8^{2-}$ and activation to $SO_4^{-}\bullet$. Nevertheless, the former process is more stable at room temperature and does not show significant degradation effects. Therefore, we usually use the latter method for the degradation of pollutants. $SO_4^{-}\bullet$ has a lone electron pair and a high redox potential ($E^0(SO_4^{-}\bullet)$ = +2.60 − +3.10 V) [52]. Therefore, it can degrade and mineralize most organic pollutants theoretically.

Sulfate radicals degrade pollutants primarily through three pathways. First, hydrogen abstraction occurs during reactions with alkanes, alcohols, ethers, and esters. Second, addition reactions are the main pathway for unsaturated alkenes. Third, electron transfer is the primary mechanism when reacting with aromatic compounds [53,54].

4 Application of HC/PS in the Degradation of Organic Pollutants

4.1 Current Status

In 2018, Choi et al. [18] first revealed the synergistic degradation effect of HC/PS: The reaction rate constant for the degradation of bisphenol A by HC/PS ($K_{HC/PS}$ = 12.7 × 10^{-3} min^{-1}) was 12.7 times higher than that of HC alone (K_{HC} = 1.0 × 10^{-3} min^{-1}) and about 2.7 times higher than that of PS alone (K_{PS} = 4.7 × 10^{-3} min^{-1}).

After that, Fedorov et al. [55–59] used HC/PS to degrade benzene series, tetracycline hydrochloride, atenolol, hydroquinone, and polycyclic aromatic hydrocarbons in marine sediments, respectively. The influence of reaction conditions (inlet pressure, temperature, pH, pollutant concentration, PS dose, etc.) and degradation path also were analyzed. In their studies, it was observed that the combination of PS and HC demonstrated the highest degradation effect. Furthermore, during the process of degradation, the main

active substances were identified as $SO_4^{\bullet -}$ and •OH. •OH exhibited reactivity towards both the aromatic ring and the lipid chain, while $SO_4^{\bullet -}$ mainly reacted with the aromatic ring.

Choi et al. [60–64] added O_3, Fe (II), H_2O_2, heterogeneous Fenton, and zero-valent iron to the HC-PS system, respectively. The degradation of oxalic acid, coomassie brilliant blue, chlorophenol, sulfamerazine, and tetracycline has achieved higher degradation efficiency than that of the HC/PS system alone, showing a broad development prospect of HC/PS treatment technology. Some representative studies of HC/PS degradation pollutants are listed in Table 3. Because of its remarkable degradation efficiency, positive synergistic effects, and extensive potential for application, the system has become a frontier hot spot in the field of water treatment. However, the current research on the treatment of organic pollutants using HC/PS primarily focuses on investigating the factors that influence the degradation effectiveness, optimizing traditional HCRs, exploring the combination of HC/PS with other physical or chemical methods, and identifying the key active substances within the system. It is important to note that the HC/PS system is still in its early stages of exploration, this is mainly reflected in the following four aspects: Firstly, the application of this system has been limited to the degradation of simulated wastewater and its potential for real wastewater has not been investigated. Secondly, the current maximum volume of HC/PS employed for wastewater degradation is 12 L, which falls significantly short of the scale required for industrial applications. Thirdly, the HCRs used in the HC/PS system are traditional types and there is a lack of research on the implementation of rotating HCRs. Last but not least, the correlation between cavitation characteristics and degradation effects has not been established, and the comprehensive design methodology for the reactor structure and associated processes has not been formulated.

Table 3: Representative studies on the degradation of pollutants by HC/PS

Year	Compounds	Process	Volume (L)	Operational condition	Time (min)	Degradation rate	Ref.
2018	Bisphenol A	HC/PS	10	P_{in} = 0.5 MPa, $C_{initial}$ = 0.044 mM, $T_{initial}$ = 50°C, pH = 6, C_{PS} = 0.7 mM	120	PS: 43.11%; HC: 11.31%; HC/PS: 78.22%	[18]
2019	Oxalic acid	HC/PS/O_3	12	P_{in} = 0.51 MPa, $C_{initial}$ = 1.11 mM, $T_{initial}$ = 50°C, pH = 6, C_{PS} = 1.11 mM, O_3: 81 g/m^3	120	PS: 55.78%; HC: 48.31%; HC/PS: 69.15%; HC/PS/O_3: 99.71%	[60]
2019	Coomassie brilliant blue	HC/KPS/H_2O_2	\	P_{in} = 7 bar, $C_{initial}$ = 20 mg/L, T = 30°C, C_{KPS} = 540 mg/l, $C_{H_2O_2}$ = 676 mg/L	60	KPS: 10.24%; KPS/H_2O_2: 36.62%; HC/KPS/H_2O_2: 99.32%	[62]
2020	Brilliant cresyl blue	HC/PS	6	Pin =1.7 bar, Cinitial = 5 g/L, Tinitial = 20°C, pH = 7, C_{PS} = 1 mM	180	PS: 10%; HC: 51.36%; HC/PS: 98.47%	[49]

(Continued)

Table 3 (continued)

Year	Compounds	Process	Volume (L)	Operational condition	Time (min)	Degradation rate	Ref.
2020	Pentachlorophenol	HC/PS/Fe(II)	\	P_{in} = 0.58 MPa, $C_{initial}$ = 37.5 μM, $T_{initial}$ = 25°C, pH = 3, C_{PS} = 0.34 mM, $C_{Fe(II)}$ =0.34 mM	60	HC/PS: 66.85%; HC/PS/Fe(II): 96.73%	[61]
2021	Atenolol	HC/PS	2	P_{in} = 0.18 MPa, $C_{initial}$ = 15 mg/L, T = 25°C, pH = 6, C_{PS} = 75 mg/L	75	PS: 1%; HC: 37.1%; HC/PS: 64.5%	[57]
2021	Tetracycline	HC/PS/Fe^0	1	P_{in} = 0.7 MPa, $C_{initial}$ = 40 mg/L, T = 25°C, pH = 3 C_{PS} = 1.4 mM, C_{Fe^0} = 40 mg/L	30	PS: 7.9%; HC: 23.9%; HC/PS: 51.12%; HC/PS/Fe^0: 97.8%	[64]
2021	Carbamazepine	HC/PS/UV/ ZnO-$ZnFe_2O_4$	5	P_{in} = 9 atm, $C_{initial}$ = 15 mg/L, pH = 4, C_{PS} = 400 mg/L, $C_{ZnO\text{-}ZnFe_2O_4}$ = 400 mg/L, UV power: 18 W	60	HC: 7.7%; HC/PS: 65.73%; HC/PS/UV/ZnO-$ZnFe_2O_4$: 98.13%	[63]
2022	Tetracycline hydrochloride	HC/PS	2	P_{in} = 0.2 MPa, $C_{initial}$ = 10 mg/L, T = 30 ± 2°C, pH = 4.7, C_{PS} = 0.1 g/l	120	HC: 44.9%; HC/PS: 92.2%	[58]
2023	hydroquinone	HC/PS	\	P_{in} = 0.2 MPa, $C_{initial}$ = 50 mg/L, pH = 7.38, C_{PS} = 1.05 mM	30	HC/PS: 91.25%; SI: 4.55	[59]
2023	Model textile dye	HC/PS	10	P_{in} = 8 kg f/cm^2, $C_{initial}$ = 100 ppm, pH = 7, C_{PMS} = 2.5 g/L	120	HC: 8.77%, (COD); PMS: 13.22%, (COD); HC/PMS: 33.41% (COD);	[65]
2023	Sulfamerazine	HC/PS	5	P_{in} = 4 bar, $C_{initial}$ = 60 ppm, $T_{initial}$ = 25°CC, pH = 5.6, C_{PS} = 0.92 mM, C_{PMS} = 0.83 mM	60	HC: 27.69%; HC/PS: 84.38%; HC/PMS: 93.85%	[66]
2023	Red 83	HC/Sulfite/ ZVI	5	P_{in} = 1.75 bar, $C_{initial}$ = 50 mg/L, $T_{initial}$ = 25°C, pH = 3, C_{PS} = 250 mg/L, C_{ZVI} = 200 mg/L Air flow: 3 L/min	60	PS: 5.26%; HC: 66.04%; HC/PS/ZVI: 87.75%	[67]

4.2 Synergy Mechanism

The activation and co-degradation principles of HC/PS technology can be summarized as follows. The activation principle of HC/PS technology may be that the substantial energy released during HC causes the breaking of the -O-O- bond of PS in solution, leading to the transformation into SO_4^{-}•.

The primary mechanism for the degradation of organic pollutants is illustrated in Fig. 5. Within the highly extreme environment (internal gas phase region) generated by HC, specific pollutants vaporize into bubbles and undergo mineralization by active free radicals. Additionally, certain pollutants undergo pyrolysis at the gas-liquid interface or experience the co-degradation of •OH generated from HC and SO_4^{-}• produced by activating PS, as well as oxidation of transient supercritical water. There is also a part of the pollutants in the liquid region. The •OH and SO_4^{-}• in the solution which are unconsumed in the first two regions degrade the pollutants. Furthermore, the mechanical effects, such as shockwaves and microjets induced by HC can disrupt the main chains of organic macromolecules and can facilitate the mixing of highly oxidizing substances (•OH, SO_4^{-}•, and H_2O_2) with the solution, thereby enhancing the reaction rate.

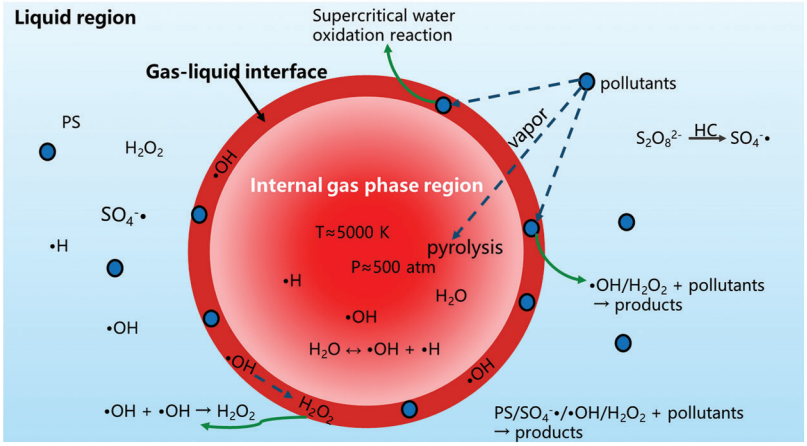

Figure 5: The synergistic degradation mechanism of the HC-PS system

5 The Main Factors of HC/PS System's Degradation Effect

Generally, the factors that mainly affect the degradation efficiency of the HC/PS system are structural parameters of HCRs, inlet pressure, reaction temperature, pH, PS concentration, and coexisting anions. The specific impact of each factor is as follows:

5.1 Structural Parameters of HCRs

For non-rotating HCRs, the throat of the venturi plays a significant role in determining its degradation effect. A stronger cavitation effect often requires a larger cavity size [68].

Agarkoti et al. [66] observed that as the residence time of the cavity in the throat increased, both the cavity volume and degradation effect increased. Their experiment revealed that the contraction angle of the Venturi had minimal impact on the degradation effect. Typically, the ratio of height/diameter to length of the throat is 1:1 and the diffusion Angle is 11 to 13° for the optimal structure. Prajapat et al. [69] also studied the degradation effects of hole plate, round venturi, and square venturi on guar gum in the HC/PS

system. The degradation effects were 89.84%, 96.26%, and 98.03% in the same condition, respectively. This can be attributed to that compared with the orifice plate and circular venturi, the square venturi has a higher flow rate and lower cavitation number so that the cycle period is shorter, the cavitation intensity is higher, and the degradation effect is better.

Li et al. [70] studied the effect of the number of holes in an orifice plate on the degradation effect of diazinon in wastewater and discovered that an appropriate increase in the number of holes could enhance the degradation effect of diazinon. However, as the number of holes continued to increase, the flow rate decreased, the cavitation number increased, and the cavitation intensity decreased. This is because reducing the number of holes can decrease the cavitation number, although the cavitation number is reduced and the cavitation effect is enhanced, the flow rate will be reduced and the cycle period will be increased. Therefore, factors such as cycle period and cavitation number should be considered when designing orifice plate HCR. In addition, the ratio of the orifice hole perimeter to its cross-sectional area (α), the ratio of hole diameter to pipe (β), and the sum of orifice hole area to pipe area ratio (β_0) are also factors to be considered in the design of orifice hole type HCRs. The influence of these factors can be specifically seen in the study of Wang et al. [19].

For rotary HCRs, the blind hole structure determines the induced cavitation intensity. Liu et al. [71] investigated the impact of blind hole structure on the cavity volume fraction based on numerical simulation and found that a blind hole with a larger aperture, deeper hole depth, and smaller inclination angle is more conducive to inducing cavitation phenomenon. Similarly, Sun et al. [72] used numerical simulation to investigate the influence of blind hole characteristics, such as shape (five kinds of structures, including cylindrical cone, cylinder, non-interacting type, cone, and hemisphere), diameter, spacing, height, and inclination, on its cavitation volume and necessary shaft power. The results demonstrated that a blind hole with a hemisphere sharp, larger diameter, smaller spacing, larger height, and larger inclination is more effective in cavitation induction and energy saving. However, there is no experimental study on the degradation of organic pollutants by rotating HCR structure at present, and the above conclusions need to be further verified.

5.2 Inlet Pressure

In general, the cavitation intensity induced by HCR demonstrates a positive correlation with the augmentation of energy input. However, it decreases after a specific threshold is reached. Therefore, in practical applications, it is important to balance the treatment effect with the energy input for each working condition. For non-rotating HCR devices, increasing the inlet pressure results in an increase in throat flow, an expansion of the downstream cavitation region, and a larger cavitation cavity region, leading to a higher cavitation intensity. Moreover, an increase in the flow rate will result in a higher number of pollutants passing through the cavitation area, enhancing the efficacy of the treatment process. However, it is worth noting that congestion cavitation may occur when the upstream pressure reaches a certain critical point [73]. This phenomenon is attributed to the merging of cavitation cavities and the formation of gas-phase cavities.

Cako et al. [49] discovered that the degradation rate of tetracycline in HC/PS increased from 2.01% to 10.07%, as the inlet pressure rose from 1.1 to 1.7 bar. Moreover, when the inlet pressure was further raised to 1.85 bar, the degradation rate dropped to 5.71%. Similarly, in the experiments conducted by Weng et al. [64], it was observed that at inlet pressures of 0.3, 0.5, and 0.7 MPa, the degradation rates were 90.38%, 97.37%, and 97%, respectively. The same conclusion was also drawn in the degradation experiment of melon gum conducted by Prajapat et al. [69].

5.3 Cavitation Number

Cavitation number is often used to express the cavitation state, which is usually related to the pressure, flow rate, and properties of the cavitation medium itself [74]. The specific expression is as follows (Eq. (1)):

$$C_v = \frac{P_2 - P_v}{(1/2)\rho v^2} \quad (1)$$

P_2: the pressure when the downstream of the cavitation reactor is fully recovered (Pa);

P_v: the saturated vapor pressure of the liquid (Pa);

V: fluid velocity (m/s).

Generally, the lower C_v, the higher cavitation intensity. This is because the number of cavities increases as the C_v decreases. Some studies have shown that the cavitation effect is significant when the $C_v < 1$. There is an optimal C_v in the degradation system. When C_v decreases further, the cavities begin to merge to form a cavity cloud, and choked cavitation occurs, thereby resulting in a reduction in cavitation intensity [44,75].

In Patil et al.'s [76] study, we found that, compared with other plates, plate B obtains lower C_v ($C_v < 1$) at all pressures and can result in stronger cavitation effects for the treatment. However, Wang [54] used HC/PS to degrade rhodamine B with different cavitation numbers and found that the degradation effect was enhanced by cavitation numbers of 0.86, 0.38, and 0.44 in that order. Kore et al. [65] also found the same result in their experiment. As the C_v decreased from 0.2959 to 0.1325, the COD removal rate increased. However, the C_v continued to decrease, the COD removal rate decreased. This phenomenon can be caused by cavitation blocking [77].

5.4 Reaction Temperature

The physical property parameters of the liquid, such as saturated vapor pressure, surface tension coefficient, density, viscosity, and concentration of dissolved gas in the liquid, are influenced by temperature [78]. These properties in turn impact the growth of cavitation (such as bubble radius and life cycle) and cavitation strength. In the HC/PS system, temperature increase has a dual effect. On the one hand, it is conducive to the activation of PS and increases the number of activated molecules in the reactants, thus accelerating the reaction rate. However, as the temperature rises, the concentration of dissolved gas in the liquid increases, resulting in the formation of excessive gas phase cavities when the cavitation bubble collapses, which reduces the cavitation intensity and degradation efficiency [79,80]. Therefore, to achieve the highest degradation rate, it is imperative to continuously optimize the experimental parameters and find the optimal reaction temperature.

Choi et al. [61] conducted a study to investigate the impact of temperature on the degradation of pentachlorophenol in the HC/PS system. They observed the kinetic rate constant of pentachlorophenol increased from 0.0285 to 0.0439 min^{-1} as the reaction temperature was increased from 20°C to 50°C. However, this finding contrasts with the results of Prajapat's [69] study, which showed a decrease in the kinetic rate constant of melon glue from 0.016 to 0.012 min^{-1} with increasing temperature. Therefore, determining the optimal reaction temperature is crucial for the HC/PS system. Furthermore, an additional cooling system must be added to the system to keep the temperature stable due to the heat generated by HC, the chemical reaction, and the pump.

5.5 pH

pH is a significant factor that influences the degradation effect of pollutants by HC/PS. In the HC-PS process, we observed that SO_4^{-}• remains stable under acidic conditions and it serves as the primary oxidizing free radical within the system (as indicated by Eqs. (2) and (3)). However, under alkaline conditions, SO_4^{-}• is consumed to generate •OH (Eq. (4)), resulting in the coexistence of SO_4^{-}• and •OH.

Furthermore, according to Table 1, we know that the half-life of SO_4^{-}• is much longer than that of •OH, and SO_4^{-}• has more sufficient time to contact with organic pollutants, which is conducive to the degradation and mineralization of organic pollutants. Moreover, the oxidation-reduction potential of SO_4^{-}• is higher than •OH, enabling SO_4^{-}• to oxidize substances that •OH is unable to oxidize [11]. However, the oxidation of SO_4^{-}• is selective and tends to react with aromatic rings, the oxidation of •OH is not selective [18,81]. Consequently, it is necessary to adjust the pH according to the characteristics of organic pollutants and possible degradation pathways.

Cako et al. [49] conducted experiments to investigate the degradation rates of BCB by the HC/PS system at various solution pH levels. The results showed that the degradation rates of BCB were 97.42%, 99.81%, 87.44%, 49.69%, 12.58%, and 37.6% at pH levels of 2, 3, 4, 5, 7, and 8, respectively. This finding suggests that both acidic and alkaline media can promote the degradation of BCB. Azizollahi et al. [67] studied the degradation of red 83 by HC/PS technology with zero-valent iron under different pH conditions. Their findings showed that the degradation rate decreased continuously as the pH increased from 3 to 9. This result can be attributed to the fact that at higher pH, Fe^{2+} is converted to Fe^{3+} in the form of precipitation, while the formation of an iron oxide film on the surface of zero-valent iron leads to a lower release of Fe^0. From the above studies, we know that the best degradation efficiency is obtained in acidic environments.

$$S_2O_8^{2-} + H^+ \rightarrow HS_2O_8^- \quad (2)$$

$$HS_2O_8^- \rightarrow SO_4\bullet^- + SO_4^{2-} + H^+ \quad (3)$$

$$SO_4\bullet^- + OH^- \rightarrow SO_4^{2-} + \bullet OH \quad (4)$$

5.6 PS Concentration

SO_4^{-}• generates from persulfate activation, so the concentration of PS is a crucial factor in the degradation of pollutants. If the PS concentration is too low, the concentration of $SO_4\bullet^-$ will be insufficient, and lead to slow reaction rates. Conversely, if the PS concentration is too high, the excess SO_4^{-}• may undergo its scavenging reactions [68], thus reducing the amount of $SO_4\bullet^-$ available for pollutant degradation. Consequently, maintaining an optimal PS concentration is essential for pollutant degradation.

Roy et al. [63] studied the degradation behavior of carbamazepine by HC/PS/UV/ZnO-$ZnFe_2O_4$ system at different PS concentrations (100–500 mg/L). The results showed that the degradation rate of PS exhibited a notable increase as the concentration of PS increased from 100 (71.92%) to 300 mg/l (91.33%). This indicates that a higher PS concentration led to a higher degradation rate of pollutants. However, when the PS concentration was further increased from 400 (96.91%) to 500 mg/l (98.13%), the degradation effect did not change significantly. This suggests that there is a saturation point beyond which increasing the PS concentration does not result in a significant improvement in the degradation rate. Weng et al. [64] conducted a study that supports the findings mentioned. They observed the degradation effect increased significantly as the PS concentration increased from 0.7 to 1.4 mM. However, when the PS concentration was further increased from 1.4 to 2.1 mM, the degradation effect remained relatively unchanged. Considering cost implications, they conduct follow-up experiments using a PS concentration of 1.4 mM. Consequently, in the actual pollutant degradation process, factors such as degradation effect and application cost must be considered and the optimal PS concentration must be selected according to the experiments.

5.7 Coexisting Anions

The presence of various anions in actual wastewater does have an impact on the degradation process of pollutants in the HC/PS system. Their presence can either enhance or hinder the degradation of pollutants, depending on their specific chemical properties and interactions with pollutants. Under normal conditions, common anions such as Cl^-, CO_3^{2-}, HCO_3^-, NO_3^-, and SO_4^{2-} can inhibit the degradation of pollutants due to their quenching effect on SO_4^-• and •OH.

Although it is generally accepted that common anions such as Cl^- inhibit the degradation of contaminants in the HC/PS system, it has also been shown that Cl^- promotes the degradation process. The research conducted by Choi et al. [18] on Bisphenol A degradation showed that Cl^- acted in contrast to the usual situation. In addition, Table 4 provides evidence that the same anion plays different roles in different systems and different pollutants. In an experiment conducted by Khajeh et al. [57], the HC/PS system was used to degrade atenolol. They observed that the presence of various anions had differing levels of inhibition on the degradation process. The order of inhibition from highest to lowest was found to be: $SO_4^{2-} > Cl^- > NO_3^-$. Similarly, the experimental investigation of HC/PS/Fe^0 degradation of tetracycline conducted by Weng et al. [64] showed that the promotion of the three anions SO_4^{2-}, Cl^- and NO_3^- to the degradation effect was also $SO_4^{2-} > Cl^- > NO_3^-$. Furthermore, Azizollahi et al. [67] investigated the degradation of Red 83 under the HC/Sulfite/ZVI system and determined the degradation rates of different ions at 15 mM. The degradation rates were found to be in the following order: $SO_4^{2-} > Cl^- > NO_3^- > HCO_3^- > CO_3^{2-}$.

Table 4: Effect of co-existing anions on degradation

Compounds	Process	Operational condition	Time (min)	Anion	K_{obs} (min^{-1})	Ref.
Bisphenol A	HC/PS	P_{in} = 0.5 MPa, $C_{initial}$ = 0.044 mM, $T_{initial}$ = 50°C, pH = 6, C_{PS} = 0.7 mM, C_{anion} = 0.32 mM.	120	None	0.0127	[18]
				Cl^-	0.027	
				HCO_3^-	0.0123	
				NO_3^-	0.0195	
Atenolol	HC/PS	P_{in} = 0.18 MPa, $C_{initial}$ = 15 mg/L, T = 25°C, pH = 6, C_{PS} =75 mg/L.	50	None	0.018	[57]
				Cl^-	0.019	
				CO_3^{2-}	0.008	
				HCO_3^-	0.009	
				NO_3^-	0.061	
				SO_4^{2-}	0.083	
				PO_4^{3-}	0.039	
Tetracycline	HC/PS/Fe^0	P_{in} = 0.5 MPa, $C_{initial}$ = 40 mg/L, T = 25°C, pH = 7, C_{PS} = 1.4 mM, C_{Fe^0} = 40 mg/L, C_{anion} = 10 mM.	30	None	0.4600	[64]
				Cl^-	0.4210	
				NO_3^-	0.3785	
				SO_4^{2-}	0.4416	
				$H_2PO_4^-$	0.4035	

(Continued)

Table 4 (continued)

Compounds	Process	Operational condition	Time (min)	Anion	K_{obs} (min^{-1})	Ref.
Red 83	HC/Sulfite/ ZVI	P_{in} = 1.75 bar, $C_{initial}$ = 50 mg/L, $T_{initial}$ = 25°C, pH = 3, C_{PS} = 250 mg/L, C_{ZVI} = 200 mg/L, Air flow: 3 L/min, C_{anion} = 15 mM.	60	None	0.035	[67]
				Cl^-	0.044	
				CO_3^{2-}	0.007	
				HCO_3^-	0.014	
				NO_3^-	0.023	
				SO_4^{2-}	0.055	

6 The Application and Concerns of HC/PS

In practical industrial applications, degradation efficiency and degradation cost are two important concerns. The degradation cost of the HC/PS system usually refers to the energy consumed by the pump and the consumption of purchasing oxidant [65].

Choi et al. [18] compared the degradation cost of HC, PS, and HC/PS systems under the same operating conditions. The cost was calculated to be 37.4, 35.4, and 20.9 \$/m^3, respectively. The degradation rates of them are 2.6, 4.7, and 12.6×10^{-3} min^{-1}, respectively. Consequently, it can be said that the HC/PS system has advantages in both treatment efficiency and degradation cost. Li et al. [59] compared the time, cavitational yield (which is defined as the pollutant degradation extent per unit energy utilized as well as the oxidant consumption.), and total cost when the hydroquinone degradation rate reached 90% in different systems. They found that the order of processing time from shortest to longest is HC/1.05 mM PS (15 min), HC/0.83 mM PS (25 min), and HC (120 min). Similarly, the order of cavitational yield from highest to lowest is HC/1.05 mM PS (1.6×10^{-4} mg/J), HC/0.83 mM PS (9.6×10^{-5} mg/J), and HC (2.53×10^{-5} mg/J). Furthermore, the order of total cost from highest to lowest is HC/1.05 mM PS (0.49 \$/m^3), HC/0.83 mM PS (0.409 \$/m^3), and HC (1.527 \$/m^3). Similarly, in Choi's [60] study on OA degradation with HC/PS/O_3 system, we can also gain the same conclusion that the combined process has the highest degradation efficiency and the lowest total application cost. Agarkoti et al. [66] also conducted an estimation of the degradation cost for HC and HC/PS systems. The study revealed that the cavitational yield of the HC/PS system is four times that of HC, but the cost of HC/PS is approximately one-fourth that of HC. It can be seen from previous studies that the HC/PS system has the advantages of low total cost, low energy consumption, and high degradation rate in practical industrial applications.

Although the HC/PS system has the advantages above in practical applications, the following aspects should be paid attention to in practical application:

(1) The heat generated by the pump, cavitation effect, and chemical reaction contribute to an increase in the reaction temperature of the system, thereby negatively impacting the degradation effect of HC/PS. To solve this, the addition of a cooling layer in the reaction pool is necessary in practical applications to maintain a relatively stable temperature.

(2) In the HC/PS system, pH plays a crucial role in determining the degradation effect. Generally, the optimal degradation effect occurs in acidic environments. However, the pH levels in acidic environments do not meet the required standards for effluent discharge. Therefore, it is necessary to adjust the pH to a neutral level after treating organic wastewater to ensure compliance with discharge requirements.

(3) Some components in real organic wastewater, such as co-existing anions, may have an inhibitory effect on the oxidative degradation of organic pollutants. Consequently, the wastewater needs to be pretreated to reduce its concentration.

7 Summary and Outlook

7.1 Summary

PS is a cheap and easily available oxidant, but it needs to be activated to form SO_4^{-}• in order to fully utilize its oxidation capabilities. HC is a novel and environmentally friendly process enhancement technique that can effectively activate persulfate. The combination of HC and PS can greatly enhance the degradation rate of organic pollutants and has the advantages of environmental friendliness, absence of pollution, and huge industrial application prospects. Based on the above analysis, the main findings of this review can be summarized as follows:

(1) The current research on the treatment of organic pollutants using HC/PS primarily focuses on investigating the factors that influence the degradation effectiveness, optimizing traditional HCRs, exploring the combination of HC/PS with other physical or chemical methods, and identifying the key active substances within the system.

(2) The mechanism of HC/PS synergistic degradation of organic pollutants lies in the oxidation of •OH, SO_4^{-}•, H_2O_2, PS, and supercritical water, pyrolysis of pollutants. Additionally, the mechanical effects induced by HC can disrupt the main chains of organic macromolecules, facilitate the mixing of highly oxidizing substances with the solution, and enhance the degradation effect.

(3) The operating parameters of the cavitation, such as structural parameters, inlet pressure, temperature, PS concentration, pH value, and co-existing anions, play a crucial role in the effective degradation of organic pollutants by HC/PS. Cavitation intensity and cycle period should be considered when selecting HCRs' structure parameters. Additionally, the optimal parameters of inlet pressure, temperature, PS concentration, pH, and coexisting anions need to be found according to the nature of the contaminant, possible degradation pathway, and cost.

7.2 Outlook

Based on the summary analysis of this paper and the author's personal experience, we recommend when using the HC/PS system for organic wastewater treatment, we need to focus on the following aspects:

(1) Scale-up study of HC/PS technology: Currently, the application of this technology is limited to laboratory scale. The application effect and economic cost of this technology on medium and large scales need further in-depth research to clarify its amplification effect.

(2) Research on real wastewater: The research of various technologies will eventually be applied to industry. However, current investigations about the degradation of wastewater using the HC/PS system primarily focus on simulated wastewater. Therefore, it is imperative to study the degradation effect of the system on real wastewater. By doing this, we can gain valuable insights into the potential application and limitations of HC/PS technology in real wastewater treatment.

(3) Research on the correlation between cavitation characteristics and degradation effect: The correlation between cavitation characteristics and degradation effect in the HC process is influenced by various structural and operational parameters of HCRs. Therefore, further investigation is needed to explore methods for optimizing the design of HCRs and regulating the parameters of the cavitation process to gain the most optimal cavitation effect.

Acknowledgement: This research is supported by the laboratory of high efficiency and clean machinery manufacturing of the ministry of education at Shandong University.

Funding Statement: The authors received no specific funding for this study.

Author Contributions: The authors confirm their contribution to the paper as follows: study conception and design: Zhu Xiufeng and Wang Jingying; data collection: Zhu Xiufeng and Wang Jingying; analysis and interpretation of results: Zhu Xiufeng and Wang Jingying; draft manuscript preparation: Zhu Xiufeng and Wang Jingying. All authors reviewed the results and approved the final version of the manuscript.

Availability of Data and Materials: The data that support the findings of this paper are available from the corresponding author upon reasonable request.

Conflicts of Interest: The authors declare that they have no conflicts of interest to report regarding the present study.

References

1. Zhang, R., Yang, S., An, Y. W., Wang, Y. Q., Lei, Y. et al. (2022). Antibiotics and antibiotic resistance genes in landfills: A review. *Science of the Total Environment, 806,* 150647.
2. Siddiqui, M. F., Khan, S. A., Hussain, D., Tabrez, U., Ahamad, I. et al. (2022). A sugarcane bagasse carbon-based composite material to decolor and reduce bacterial loads in waste water from textile industry. *Industrial Crops & Products, 176,* 114301.
3. Liu, J. Y., Liu, L. H., Xue, J. R., Lv, C. Q., Li, T. et al. (2018). Research progress of adsorption treatment of heavy metal wastewater. *Environmental Chemistry, 37(9),* 2016–2024.
4. Lv, H. L., Liu, D. Q. (2006). Review on treatment technology of industrial wastewater. *Environmental Protection of Petrochemical Industry, 29(4),* 15–19.
5. Chui, C. M., Chen, H. Y., Lee, C. H., Hong, P. K. A., Yang, P. Y. et al. (2021). Immobilized biological method for anaerobic biodegradation of carbohydrate and protein in wastewater. *Environmental Technology & Innovation, 22,* 101431.
6. Yang, L., Xu, X., Wang, H., Yan, J., Ren, N. et al. (2022). Biological treatment of refractory pollutants in industrial wastewaters under aerobic or anaerobic condition: Batch tests and associated microbial community analysis. *Bioresource Technology Reports, 17,* 100927.
7. Li, W., Mu, B., Yang, Y. (2019). Feasibility of industrial-scale treatment of dye wastewater via bio-adsorption technology. *Bioresource Technology, 277,* 157–170.
8. Shrivastava, V., Ali, I., Marjub, M. M., Rene, E., Soto, A. M. F. (2022). Wastewater in the food industry: Treatment technologies and reuse potential. *Chemosphere, 293,* 133553.
9. Liu, L. M., Chen, Z., Zhang, J. W., Shan, D., Wu, Y. et al. (2021). Treatment of industrial dye wastewater and pharmaceutical residue wastewater by advanced oxidation processes and its combination with nanocatalysts: A review. *Journal of Water Process Engineering, 42,* 102122.
10. Glaze, W. H., Kang, J. W., Chapin, D. H. (1987). The chemistry of water treatment processes involving ozone hydrogen peroxide and ultraviolet radiation. *Ozone: Science & Engineering, 9(4),* 335–352.
11. Lee, J., Gunten, U. V., Kim, J. H. (2020). Persulfate-based advanced oxidation: Critical assessment of opportunities and roadblocks. *Environmental Science & Technology, 54(6),* 3064–3081.
12. Tan, C. Q., Gao, N. Y., Deng, Y., Rong, W. L., Zhou, S. D. et al. (2013). Degradation of antipyrine by heat activated persulfate. *Separation and Purification Technology, 109,* 122–128.
13. Tan, C. Q., Gao, N. Y., Chu, W. H., Li, C., Templeton, M. R. (2012). Degradation of diuron by persulfate activated with ferrous ion. *Separation and Purification Technology, 95,* 44–48.
14. Hao, F. F., Guo, W. L., Wang, A. Q., Leng, Y. Q., Li, H. L. (2014). Intensification of sonochemical degradation of ammonium perfluorooctanoate by persulfate oxidant. *Ultrasonics Sonochemistry, 21(2),* 554–558.

15. Chen, L. W., Cai, T. M., Cheng, C., Xiong, Z., Ding, D. H. (2018). Degradation of acetamiprid in UV/H_2O_2 and UV/persulfate systems: A comparative study. *Chemical Engineering Journal, 351,* 1137–1146.
16. Dominguez, C. M., Rodriguez, V., Montero, E., Romero, A., Santos, A. (2020). Abatement of dichloromethane using persulfate activated by alkali: A kinetic study. *Separation and Purification Technology, 241,* 116679.
17. Lebik-Elhadi, H., Frontistis, Z., Ait-Amar, H., Madjene, F., Mantzavinos, D. (2020). Degradation of pesticide thiamethoxam by heat-activated and ultrasound-activated persulfate: Effect of key operating parameters and the water matrix. *Process Safety and Environmental Protection, 134,* 197–207.
18. Choi, J., Cui, M., Lee, Y., Kim, J., Son, Y. et al. (2018). Hydrodynamic cavitation and activated persulfate oxidation for degradation of bisphenol A: Kinetics and mechanism. *Chemical Engineering Journal, 338,* 323–332.
19. Wang, B., Su, H., Zhang, B. (2021). Hydrodynamic cavitation as a promising route for wastewater treatment–A review. *Chemical Engineering Journal, 412,* 128685.
20. Wu, Z., Tagliapietra, S., Giraudo, A., Martina, K., Cravotto, G. (2019). Harnessing cavitational effects for green process intensification. *Ultrasonics Sonochemistry, 52,* 530–546.
21. Lakshmi, N. J., Gogate, P. G., Pandit, A. B. (2021). Treatment of acid violet 7 dye containing effluent using the hybrid approach based on hydrodynamic cavitation. *Process Safety and Environmental Protection, 153,* 178–191.
22. Ranade, N. V., Nagarajan, S., Sarvothaman, V., Ranade, V. V. (2021). ANN based modelling of hydrodynamic cavitation processes: Biomass pre-treatment and wastewater treatment. *Ultrasonics Sonochemistry, 72,* 105428.
23. Flint, E. B., Suslick, K. S. (1991). The temperature of cavitation. *Science, 253,* 1397–1399.
24. Dijkink, R., Ohl, C. (2008). Measurement of cavitation induced wall shear stress. *Applied Physics Letters, 93(25),* 254107.
25. Holzfuss, J., Rüggeberg, M., Billo, A. (1998). Shock wave emissions of a sonoluminescing bubble. *Physical Review Letters, 81(24),* 5434–5437.
26. Philipp, A., Lauterborn, W. (1998). Cavitation erosion by single laser-produced bubbles. *Journal of Fluid Mechanics, 361,* 75–116.
27. Bang, J. H., Suslick, K. S. (2010). Applications of ultrasound to the synthesis of nanostructured materials. *Advanced Materials, 22(10),* 1039–1059.
28. Lv, X. P., Ding, D. S., Zhang, P. (2020). *Ultrasonic chemical process strengthening*. China: Chemical Industry Press.
29. Entzian, K., Aigner, A. (2021). Drug delivery by ultrasound-responsive nanocarriers for cancer treatment. *Pharmaceutics, 13,* 1135.
30. Yasuda, K. (2021). Sonochemical green technology using active bubbles: Degradation of organic substances in water. *Current Opinion in Green and Sustainable Chemistry, 27,* 100411.
31. Jiang, Z., Li, Y., Wang, S., Cui, C., Yang, C. et al. (2020). Review on mechanisms and kinetics for supercritical water oxidation processes. *Applied Sciences, 10,* 4937.
32. Fedorov, K., Dinesh, K., Sun, X., Soltani, R. D. C., Wang, Z. H. et al. (2022). Synergistic effects of hybrid advanced oxidation processes (AOPs) based on hydrodynamic cavitation phenomenon—A review. *Chemical Engineering Journal, 432,* 134191.
33. Gogate, P. R., Pandit, A. B. (2001). Hydrodynamic cavitation reactors: A state of the art review. *Reviews in Chemical Engineering, 17(1),* 1–85.
34. Carpenter, J., Pinjari, D. V., Saharan, V. K., Pandit, A. B. (2022). Critical review on hydrodynamic cavitation as an intensifying homogenizing technique for oil-in-water emulsification: Theoretical insight, current status, and future perspectives. *Industrial & Engineering Chemistry Research, 61,* 10587–10602.
35. Zhang, W., Xie, C., Fan, H., Liu, B. (2022). Influence of hole geometry on performance of a rotational hydrodynamic cavitation reactor. *Frontiers in Energy Research, 10,* 881811.
36. Joshi, J. B., Pandit, A. B. (1993). Hydrolysis of fatty oils: Effect of cavitation. *Chemical Engineering Science, 48,* 3440–3442.

37. Sivakumar, M., Pandit, A. B. (2001). Hydrodynamic cavitation assisted rhodamine B degradation: A technologically viable waste water treatment technique. *International Conference on Science and Technology*, pp. 12–13. New Delhi, India.
38. Kalumuck, K. M., Chahine, G. L. (2000). The use of cavitating jets to oxidize organic compounds in water. *Journal of Fluids Engineering, 122(3),* 465–470.
39. Zhu, W. M., Wu, C. D., Chen, L. J., Wu, G. Z. (2007). Study on the influence factors of phenol degradation in water by ozone enhanced by hydraulic cavitation. *Industrial Water and Wastewater, 2,* 23–26.
40. Wang, X. K., Zhang, Y. (2009). Degradation of alachlor in aqueous solution by using hydrodynamic cavitation. *Journal of Hazardous Materials, 161(1),* 202–207.
41. Saharan, V. K., Pandit, A. B., Kumar, P. S. S., Anandan, S. (2012). Hydrodynamic cavitation as an advanced oxidation technique for the degradation of acid red 88 dye. *Industrial & Engineering Chemistry Research, 51(4),* 1981–1989.
42. Parsa, J. B., Zonouzian, S. A. Z. (2013). Optimization of a heterogeneous catalytic hydrodynamic cavitation reactor performance in decolorization of Rhodamine B: Application of scrap iron sheets. *Ultrasonics Sonochemistry, 20(6),* 1442–1449.
43. Patil, P. N., Bote, S. D., Gogate, P. R. (2014). Degradation of imidacloprid using combined advanced oxidation processes based on hydrodynamic cavitation. *Ultrasonics Sonochemistry, 21(5),* 1770–1777.
44. Rajoriya, S., Bargole, S., Saharan, V. K. (2017). Degradation of reactive blue 13 using hydrodynamic cavitation: Effect of geometrical parameters and different oxidizing additives. *Ultrasonics Sonochemistry, 37,* 192–202.
45. Barik, A. J., Gogate, P. R. (2018). Hybrid treatment strategies for 2,4,6-trichlorophenol degradation based on combination of hydrodynamic cavitation and AOPs. *Ultrasonics Sonochemistry, 40,* 383–394.
46. Tao, Y. Q., Cai, J., Huai, X. L., Liu, B. (2017). A novel device for hazardous substances degradation based on double-cavitating-jets impingement: Parameters optimization and efficiency assessment. *Journal of Hazardous Materials, 335,* 188–196.
47. Wang, X. N., Jia, J. P., Wang, Y. L. (2017). Combination of photocatalysis with hydrodynamic cavitation for degradation of tetracycline. *Chemical Engineering Journal, 315,* 274–282.
48. Wang, C. Q., Jin, R. Y., He, Z. D., Qiao, Y. N., Wang, Y. et al. (2020). A new water treatment technology for degradation of B[a]A by hydrodynamic cavitation and chlorine dioxide oxidation. *Ultrasonics Sonochemistry, 61,* 104834.
49. Cako, E., Gunasekaran, K. D., Soltani, R. D. C., Boczkaj, G. (2020). Ultrafast degradation of brilliant cresyl blue under hydrodynamic cavitation based advanced oxidation processes (AOPs). *Water Resources and Industry, 24,* 100134.
50. Patil, P. B., Thanekar, P., Bhandari, V. M. (2023). A strategy for complete degradation of metformin using vortex-based hydrodynamic cavitation. *Industrial & Engineering Chemistry Research, 62,* 19262–19273.
51. Pereira, T. C., Flores, E. M. M., Abramova, A. V., Verdini, F., Gaudino, E. C. et al. (2023). Simultaneous hydrodynamic cavitation and glow plasma discharge for the degradation of metronidazole in drinking water. *Ultrasonics Sonochemistry, 95,* 106388.
52. Oh, W. D., Dong, Z. L., Lim, T. T. (2016). Generation of sulfate radical through heterogeneous catalysis for organic contaminants removal: Current development, challenges and prospects. *Applied Catalysis B: Environmental, 194,* 169–201.
53. Minisci, F., Citterio, A. (1983). Electron-transfer processes: Peroxydisulfate, a useful andversatile reagent in organic chemistry. *Accounts of Chemical Research, 16,* 27–32.
54. Wang, Q. (2018). *Study on the efficiency and mechanism of hydrocavitation enhanced persulfate oxidation in the treatment of dye wastewater.* China: Zhejiang Gongshang University.
55. Fedorov, K., Sun, X., Boczkaj, G. (2021). Combination of hydrodynamic cavitation and SR-AOPs for simultaneous degradation of BTEX in water. *Chemical Engineering Journal, 417,* 128081.
56. Hung, C. M., Huang, C. P., Chen, C. W., Hsieh, S., Dong, C. D. (2021). Remediation of contaminated dredged harbor sediments by combining hydrodynamic cavitation, hydrocyclone, and persulfate oxidation process. *Journal of Hazardous Materials, 420,* 126594.

57. Khajeh, M., Amin, M. M., Fatehizadeh, A., Aminabhavi, J. M. (2021). Synergetic degradation of atenolol by hydrodynamic cavitation coupled with sodium persulfate as zero-waste discharge process: Effect of coexisting anions. *Chemical Engineering Journal, 416,* 129163.
58. Wang, B. W., Wang, T. T., Su, H. J. (2022). Hydrodynamic cavitation (HC) degradation of tetracycline hydrochloride (TC). *Separation and Purification Technology, 282,* 120095.
59. Li, X. H., Long, Z. Y., Li, X. B. (2023). Hydrodynamic cavitation degradation of hydroquinone using swirl-type micro-nano bubble reactor. *Environmental Technology, 2,* 248557.
60. Choi, J., Cui, M., Lee, Y., Ma, J., Kim, J. et al. (2019). Hybrid reactor based on hydrodynamic cavitation, ozonation, and persulfate oxidation for oxalic acid decomposition during rare-earth extraction processes. *Ultrasonics Sonochemistry, 52,* 326–335.
61. Choi, J., Cui, M., Lee, Y., Kim, J., Son, Y. et al. (2020). Application of persulfate with hydrodynamic cavitation and ferrous in the decomposition of pentachlorophenol. *Ultrasonics Sonochemistry, 66,* 105106.
62. Baradaran, S., Sadeghi, M. T. (2019). Coomassie Brilliant Blue (CBB) degradation using hydrodynamic cavitation, hydrogen peroxide and activated persulfate (HC-H_2O_2-KPS) combined process. *Chemical Engineering and Processing Process Intensification, 145,* 107674.
63. Roy, K., Moholkar, V. S. (2021). Mechanistic analysis of carbamazepine degradation in hybrid advanced oxidation process of hydrodynamic cavitation/UV/persulfate in the presence of ZnO/$ZnFe_2O_4$. *Separation and Purification Technology, 270,* 118764.
64. Weng, M. T., Cai, M. Q., Xie, Z. Q., Dong, C. Y., Zhang, Y. et al. (2022). Hydrodynamic cavitation enhanced heterogeneous activation of persulfate for tetracycline degradation: Synergistic effects, degradation mechanism and pathways. *Chemical Engineering Journal, 431(3),* 134238.
65. Kore, V. S., D.Manjare, S., D.Patil, A., Dhanke, B. P. (2023). A parametric study on intensified degradation of textile dye water using hydrodynamic cavitation based hybrid technique. *Chemical Engineering and Processing-Process Intensification, 193,* 109550.
66. Agarkoti, C., Gujar, S. K., Gogate, P. R., Pandit, A. B. (2023). Pilot scale degradation of Sulfamerazine using different venturi based hydrodynamic cavitation and ultrasound reactors in combination with oxidation processes. *Journal of Environmental Chemical Engineering, 11(3),* 109857.
67. Azizollahi, N., Taheri, E., Amin, M. M., Rahimi, A., Fatehizadeh, A. et al. (2023). Hydrodynamic cavitation coupled with zero-valent iron produces radical sulfate radicals by sulfite activation to degrade direct red 83. *Ultrasonics Sonochemistry, 95,* 106350.
68. Agarkoti, C., Thanekar, P. D., Gogate, P. R. (2021). Cavitation based treatment of industrial wastewater: A critical review focusing on mechanisms, design aspects, operating conditions and application to real effluents. *Journal of Environmental Management, 300,* 113786.
69. Prajapat, P. L., Gogate, P. R. (2015). Intensification of depolymerization of aqueous guar gum using hydrodynamic cavitation. *Chemical Engineering and Processing: Process Intensification, 93,* 1–9.
70. Li, B. Q., Li, S., Yi, L. D., Sun, H. S., Qin, J. et al. (2021). Degradation of organophosphorus pesticide diazinon by hydrodynamic cavitation: Parameters optimization and mechanism investigation. *Process Safety and Environmental Protection, 153,* 257–267.
71. Liu, Y., Li, X. L., Chen, T. R., Wang, G. Y., Huang, B. (2017). Numerical study on the cavitating flow in a rotary cavitation generator. *Transaction of Beijing Institute of Technology, 37(1),* 1–4+14.
72. Sun, X., You, W. B., Xuan, X. X., Ji, L., Xu, X. T. et al. (2021). Effect of the cavitation generation unit structure on the performance of an advanced hydrodynamic cavitation reactor for process intensifications. *Chemical Engineering Journal, 412,* 128600.
73. Saharan, V. K., Badve, M. P., Pandit, A. B. (2011). Degradation of reactive red 120 dye using hydrodynamic cavitation. *Chemical Engineering Journal, 178,* 100–107.
74. Gogate, P. R. (2008). Cavitational reactors for process intensification of chemical processing applications: A critical review. *Chemical Engineering and Processing: Process Intensification, 47(4),* 515–527.
75. Patil, A., Baral, A., Dhanke, P. (2021). Hydrodynamic cavitation for process intensification of biodiesel synthesis–A review. *Current Research in Green and Sustainable Chemistry, 4,* 100144.

76. Patil, A. D., Baral, A. S. (2021). Process intensification of thumba methyl ester (Biodiesel) production using hydrodynamic cavitation. *Chemical Engineering Research and Design, 171,* 277–292.
77. Rajoriya, S., Carpenter, J., Saharan, V. K., Pandit, A. B. et al. (2016). Hydrodynamic cavitation: An advanced oxidation process for the degradation of bio-refractory pollutants. *Reviews in Chemical Engineering, 32(4),* 379–411.
78. Mohod, A. V., Gogate, P. R. (2011). Ultrasonic degradation of polymers: Effect of operating Parameters and intensification using additives for carboxymethyl cellulose (CMC) and polyvinyl alcohol (PVA). *Ultrasonics Sonochemistry, 18(3),* 727–734.
79. Patil, P. N., Gogate, P. R. (2012). Degradation of methyl parathion using hydrodynamic cavitation: Effect of operating parameters and intensification using additives. *Separation and Purification Technology, 95,* 172–179.
80. Gogate, P. R., Patil, P. N. (2015). Combined treatment technology based on synergism between hydrodynamic cavitation and advanced oxidation processes. *Ultrasonics Sonochemistry, 25,* 60–69.
81. Molkenthin, M., Olmez-Hanci, T., R.Jekel, M., Arslan-Alaton, I. (2013). Photo-Fentonlike treatment of BPA: Effect of UV light source and water matrix on toxicity and transformation products. *Water Research, 47(13),* 5052–5064.